

**(IS-CFAR) - Aided Complex Wavelet De-noising**

Dr. Riyadh Ali Abdulhussein, Hussein M. Hathal, Sarmad K. Ibrahim

Al-Mustansiriyah University, College of Engineering, Electrical Engineering Department, Baghdad, Iraq  
[Riyadh\\_alhilali@yahoo.com](mailto:Riyadh_alhilali@yahoo.com), [hussat@gmail.com](mailto:hussat@gmail.com), [sarmad\\_8888@yahoo.com](mailto:sarmad_8888@yahoo.com)

**Abstract:** A novel use of the complex wavelet transform (CWT) for the study and application in the de-noising of radar signals is presented in the main part of the paper. This paper includes an application of complex wavelet transform (CWT) in de-noising problem of noise smoothing for reference cells. Since, complex wavelet transform has significant advantages over real wavelet transform for de-noising problem. In this paper another technique is added to Improved Switching – Constant False Alarm Rate (IS-CFAR) algorithm to further reduce the effects of the non-homogenous and clutter wall, since CFAR detectors are commonly used in modern radar detection systems. In radar systems, the target is isolated from noise by setting detection thresholds through using CFAR algorithms, thus keeping the false alarm rate at certain level. The main goal of the paper is to show the de-noising algorithm based upon the complex wavelet transform (CWT) that can be applied successfully to enhance noise removal. The simulation tests presented detection performance of (IS-CFAR) improvement system by employing complex wavelet de-noising for homogenous and non-homogenous cases. Simulation results demonstrate that the Complex Discrete Wavelet Transform based de-noising outperforms conventional discrete wavelet de-noising. Approximately access gains in SNR about (1.2) dB and (2.3) dB are achieved compared with (IS-CFAR) system with homogeneous environment, swerling II and III cases for the same probability of detection.

[Dr. Riyadh Ali Abdulhussein, Hussein M. Hathal, Sarmad K. Ibrahim. **(IS-CFAR) - Aided Complex Wavelet De-noising**. *J Am Sci* 2014;10(11):185-190]. (ISSN: 1545-1003). <http://www.jofamericanscience.org>. 25

**Keywords:** CFAR; IS-CFAR; discrete wavelet transform (DWT); complex discrete wavelet transform (CDWT); de-noising; reference cells.

**1. Introduction**

A radar detection process involves testing whether the signal level in the resolution cell under test exceeds a detection threshold. In modern radar systems, the detection threshold is adaptively adjusted according to the background clutter and noise levels using a constant false alarm rate (CFAR) processor [1]. The main objective in target detection is to maximize the target detection probability under the constraints of very low and Constant False Alarm Rate (CFAR). Thus, CFAR is a set of techniques designed to provide predictable detection and false alarm behavior in realistic interference scenarios. Attractive classes of schemes that can be used to overcome the problem of clutter are the (CFAR) processing schemes which set the threshold adaptively based on local information of total noise power.

The goal of CFAR algorithms is reliably estimate the main noise and scaling the estimated mean by a multiplier to obtain the threshold set high enough false alarm rate to a tolerably small rate [2].

Performance analysis of various CFAR schemes focuses on whether the sample false alarm rate remains constant. Thus, in order to compare CFAR schemes in various clutter environments, a comparison of false alarm probabilities is required [3].

The probability of false alarm, PFA, is the chance that spikes in noise or clutter is mistaken by the CFAR algorithm as a target.

As noise and clutter distributions are continuous, extending from amplitudes very close to zero to amplitudes extending infinitely outwards [2].

The mean level detector, as in 1998, is the most basic forms of the adaptive detection processors. A new adaptive coherent CFAR wavelet detector which can be used as an additional independent detector for effective CFAR detection of point targets [4], in 2005 another preprocessing approaches based on a non-linear compressing filter to reduce the noise effect [5]. A CFAR detector based on de-noising via wavelet shrinkage is appeared in 2007 [6], while improved the switching CFAR (S-CFAR) appeared in 2008 so as to fix the false alarm rate (FAR) not only in the homogenous environment with thermal noise but also in a non-homogenous environment. S-CFAR selects different reference cells to compute the detection threshold by using the magnitude of the test cell; also S-CFAR exhibits a good performance in homogeneous environments and multiple targets situations but suffers from excessive false alarm rates in clutter edge environments [7].

In 2013 a new composite of CFAR processor also known as Improved Switching CFAR (IS-CFAR). IS-CFAR exhibits a lower CFAR loss than S-CFAR in a homogeneous environment and performs almost the same detection performance as S-CFAR in a multiple targets situation. At a clutter edge, the false

alarm rate of IS-CFAR is much lower than that of S-CFAR [8].

The paper presents the theory of the fundamental mathematical tool complex wavelet transform (CWT) that is used for the signal processing of CFAR algorithm, wavelet transform is widely used in many signal processing applications. Also, it has been used in radar signal detection, such as target detection, clutter suppression and CFAR detection [6]. The wavelet shrinkage is a powerful approach for smoothness. Wavelet analysis is simply the process of decomposing a signal into shifted and scaled versions of a mother (initial) wavelet. An important property of wavelet analysis is perfect reconstruction, which is the process of reassembling a decomposed signal or image into.

The smoothing algorithm can be implemented using discrete wavelet transform (DWT). By restricting to a discrete set of parameters, one can get the Discrete Wavelet Transform (DWT) [9] which corresponds to an orthogonal basis of functions all derived from a single function called the mother wavelet. The discrete wavelet transform (DWT) [10] is another way to decompose a time series into a sequence of components with different scales. The original signal can be reconstructed from these components. In this study instead of conventional discrete wavelet transform, the Complex Discrete Wavelet Transform was used for de-noising signals.

**2. CFAR Detector**

In IS-CFAR method, the reference cells is divided into the leading window and lagging windows. Each of windows A and B contained from N/2 reference cells, as illustrated in Fig.(1) [8]. In CFAR, the samples of received signal are passed through a square-law detector (SLD) and stored in a shift register. The middle of the shift register is the cell under test (CUT) and denoted by  $X_0$ . Reference cells are combined to yield an estimate  $Z$  of the noise level in CUT. The CUT is then compared with the adaptive threshold i.e.  $T = \alpha Z$  to decide about the existence of the target:

$$X_0 \begin{matrix} \geq T & H_1 \\ & \\ \leq T & H_0 \end{matrix}$$

Where  $H_1$  and  $H_0$  are the hypothesis of existence and nonexistence of the target, respectively, and the scaling factor  $\alpha$  is selected to set a desired false alarm probability. In IS-CFAR, a comparison threshold is generated by multiplying the amplitude of the test cell by a scaling factor. Then in the leading and lagging reference windows, the numbers of reference cells whose amplitudes are smaller than the comparison threshold are counted and compared with a threshold integer respectively. The detection threshold

is computed by selecting appropriate reference cells based on the comparison result.

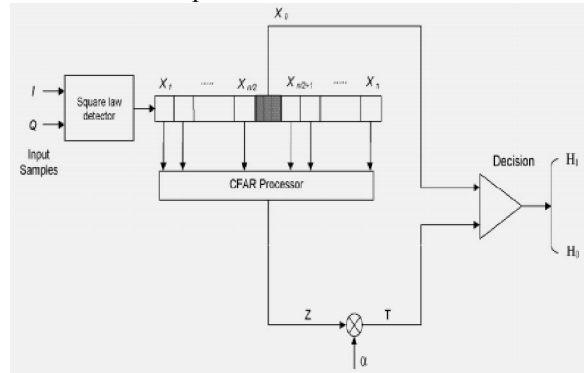


Fig. 1. Typical CFAR detector

**3. Improved Switching (IS-CFAR) Algorithm**

The block diagram of proposed IS-CFAR is shown in Fig. 2. In IS-CFAR method, the reference window is divided into the leading (called A for simplification) and lagging windows (called B for simplification). Each of windows A and B contains N reference cells. Since, the amplitude of the target return presented in the tapped line fluctuates according to the Swerling I model [8], The reference cells in window A and B are partitioned into two sets  $S_{0,A/B}$  and  $S_{1,A/B}$ , respectively. A comparison stage between the amplitude of each reference cell and the comparison threshold  $\alpha X_0$  is done with assuming that  $n_{0,A}$  and  $n_{0,B}$  denote the numbers of cells contained in  $S_{0,A}$  and  $S_{0,B}$ , respectively. The detection threshold ( $Th$ ) of IS-CFAR is computed by selecting appropriate reference cells.

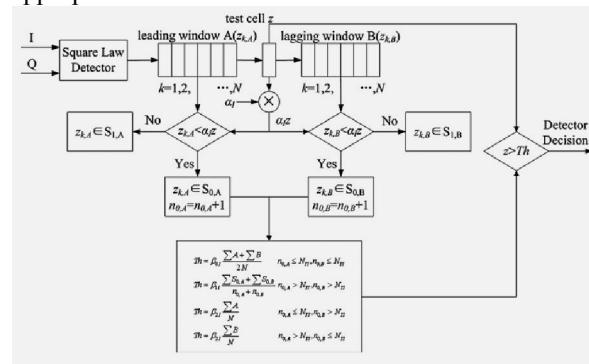


Fig. 2. IS-CFAR block diagram

Where,  $N_T$ , is threshold integer,  $n_{0,A}$ , and  $n_{0,B}$  are the number of reference cells stored in  $S_{0,A}$  and  $S_{0,A}$  respectively.

The main problem of CFAR detection is non-homogeneities. Since, two kinds of non-homogeneities, i.e. interfering targets and clutter-edge are considered. Interfering targets are strong signals related to targets appeared in reference cells and cause an incorrect estimation of the level of the noise in

CFAR processor and so decrease the probability of detection. While, clutter-edge is the situation in which power of the clutter in reference cells changes from one level to another level, instantaneously. Also, it causes an incorrect estimation of the level of the noise and changes the probability of false alarm [6].

If the test cell contains thermal noise only, then there is no matter the reference window contains interfering targets or not. In order to maintain a low false alarm rate, all of the reference cells are selected to estimate the background noise/clutter power. If the test cell contains a target return with a high SNR, then there is a high probability that the noise cells in window A and B are partitioned into  $S_{0,A}$  and  $S_{0,B}$  while the interferers are partitioned into  $S_{1,A}$  and  $S_{1,B}$ . [8]

The probability of detection ( $p_d$ ) in non-homogenous environment is derived calculated by the system of equations [8]. In order to improve the  $P_d$  in a multiple targets situation, the cells in  $S_{0,A}$  and  $S_{0,B}$  are selected to compute the detection threshold. The worst case which results in the highest false alarm rate is that the test cell contains a clutter return and is at the edge of noise and clutter regions. The false alarm rate in this situation is called the false alarm peak.

#### 4. Why Complex Wavelet Transform

Wavelet techniques are successfully applied to various problems in signal and image processing. Data compression [11], motion estimation [12], segmentation and classification [13, 14] and denoising [15] are only some examples. In spite of its efficient computational algorithm, the wavelet transform suffers from these disadvantages; shift variance, poor directionality, absence of phase information, oscillations, aliasing, and lack of directionality, these considerably complicate wavelet-based processing.

There is a simple solution to these DWT problems through noting that the Fourier transform does not suffer from these problems. First, the magnitude of the Fourier transform does not oscillate positive and negative but rather provides a smooth positive envelope in the Fourier domain. Second, the magnitude of the Fourier transform is perfectly shift invariant, with a simple linear phase offset encoding the shift. Third, the Fourier coefficients are not aliased and do not rely on a complicated aliasing cancellation property to reconstruct the signal; and fourth, the sinusoids of the Fourier basis are highly directional plane waves.

Unlike the DWT, which is based on real-valued oscillating wavelets, the Fourier transform is based on complex-valued oscillating sinusoids as with the Fourier transform, complex wavelets can be used to analyze and represent both real-valued signals (resulting in symmetries in the coefficients) and

complex-valued signals. In either case, the CWT enables new coherent multiscale signal processing algorithms that exploit the complex magnitude and phase.

The difficulties in designing complex filters limit the wide use of complex wavelets, thus to overcome this, a dual-tree implementation of the CWT is proposed which uses two trees of real filters to generate the real and imaginary parts of the wavelet coefficients separately. The two trees are shown in Fig. 3 for 1-D signals, complex wavelet coefficients are estimated by dual tree algorithm and their magnitude is shift invariant. Even though the outputs of each tree are down sampled by summing the outputs of the two trees during reconstruction so as to suppress the aliased components of the signal and achieve approximate shift invariance.

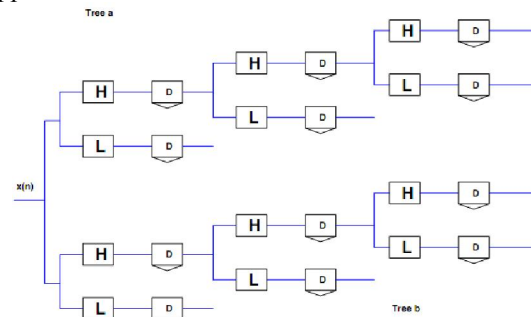


Fig.3. The 1-D dual-tree wavelet transform is implemented with a pair of filter banks operating on the same data simultaneously.

#### 5. (IS-CFAR) based on Complex Wavelet Denoising

Fig. 4 shows the complex-wavelet de-noising block diagram. The estimation of probability of detection for a given probability of false alarm  $P_{fa}$ , is determined by inputting complex-valued data  $S(x + iz)$  into the complex wavelet de-noising block, where the activity value  $S_1$  and  $S_2$  are converted into their real and imaginary parts. Daubechies 2 function is selected and applied with four levels decomposition in the complex discrete wavelet de-noising block since it has simple computational complexity, after that, the soft threshold of de-noising is chosen which shrinks complex wavelet coefficients. Signal reconstruction is done by the third operator i.e. inverse complex wavelet transform (ICWT) which uses all properties of complex wavelet transform (CWT) block. Thus, each one of ICWT block output real and imaginary values.

The implementation of IS-CFAR with the aid of complex wavelet de-noising can be depicted in Fig. 5. The algorithm passes through two stages; first, the de-noised free signal  $X$  which contains target only is subtracted from the input signal  $S$ . Second, the result

of first stage is applied to the square low detector (SLD). The input signal is used as the cell under test of the shift register.

In order to achieve the same probability of false alarm for the IS-CFAR-aided complex wavelet de-noising, then the scaling factor  $\beta$  is properly chosen so that to give the required improvements.

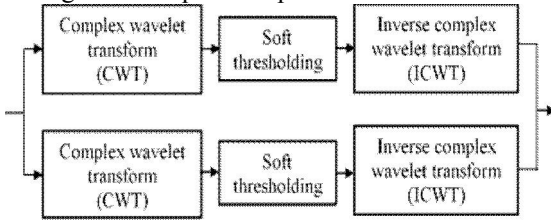


Fig. 4. Complex wavelet de-noising diagram

**6. (IS-CFAR) Algorithm Assisted Complex Wavelet De-noising**

The estimation algorithm of probability of detection for (IS-CFAR) – aided complex wavelet de-noising system can be simulated through the following steps:

1. Begin
2. Initialization step

This step sets the following parameters; complex wavelet mother function, method of shrinkage, number of iteration, window size, threshold integer, scale factor, level of decomposition.

3. Apply the complex wavelet decomposition
4. Apply filtering and threshold selection.
5. Apply inverse complex wavelet decomposition.

6. Apply subtraction the result of step 5 from the input signal.

7. Apply the SLD
8. Apply IS-CFAR criteria
9. Scaling the result of step 8 by  $\beta$  factor.

10. Compare the computed threshold for every reference window with cell under test (CUT), then;

- ❖ If (CUT) is greater than threshold, then the summation is found for all iterations.
- ❖ Compute the probability of false alarm.
- ❖ If (CUT) is smaller than threshold, then return to step 3 and continue until (CUT) becomes greater than threshold.

11. Stop

The flow chart of (IS-CFAR) algorithm assisted complex wavelet de-noising is shown in Fig. 6.

**7. Simulation Results**

After calculation the CFAR parameters, the relationship between scaling factor  $\beta$  and the probability of false alarm is determined. In this case initial values of  $\beta$  are assumed to deduce this relationship. The reference cells are corrupted by (AWGN) signal, and assuming that the signal distribution is exponential for case swerling II, and

chi-square for case swerling III. For simplicity, Stein's Unbiased Estimation (SURE) shrinkage method is used.

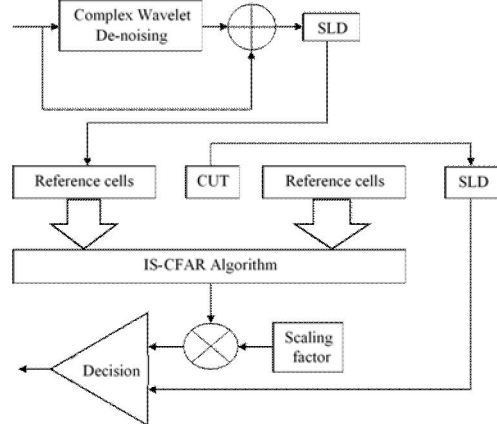


Fig. 5. (IS-CFAR) - Assisted Complex wavelet de-noising block diagram

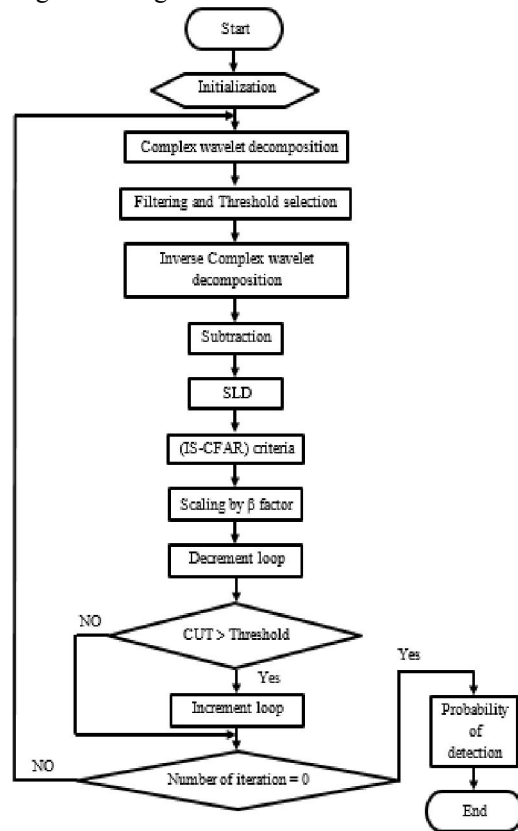


Fig. 6. Flow chart of (IS-CFAR) algorithm - Aided Complex wavelet de-noising

Assuming case swerling II is applied and the number of reference cells ( $N = 24$ ), SURE de-noising method is used, wavelet family is dB2, number of trial ( $N_{\text{trial}} = 10^5$ ), and the values of  $\alpha$  takes the range;  $(1/3) < \alpha < 1$ . For the (IS-CFAR) but without applying wavelet de-noising, Table (1) shows the calculated  $\beta$  values in range of  $\alpha$  values with respect to probability

of false alarm  $P_{fa} = 10^{-5}$ . While Table (2) shows the calculated  $\beta$  values in range of  $\alpha$  values with respect to probability of false alarm  $P_{fa} = 10^{-6}$ .

Table (1) :  $\alpha$  and  $\beta$  values at  $P_{fa} = 10^{-5}$

$\alpha$	0.333	0.5	0.7	0.9
$\beta$	16.32	17.12	17.8	18.09

Table (2) :  $\alpha$  and  $\beta$  values at  $P_{fa} = 10^{-6}$

$\alpha$	0.333	0.5	0.7	0.9
$\beta$	21.175	22.5	23.57	24.01

The values of  $\alpha$  and  $\beta$  for (IS-CFAR)-aided complex wavelet de-noising at  $P_{fa} = 10^{-5}$  and  $P_{fa} = 10^{-6}$  is shown in Table (3) and Table (4) respectively.

Table (3) :  $\alpha$  and  $\beta$  values at  $P_{fa} = 10^{-5}$

$\alpha$	0.333	0.5	0.7	0.9
$\beta$	16.8	14.4	16	18.1

Table (4) :  $\alpha$  and  $\beta$  values at  $P_{fa} = 10^{-6}$

$\alpha$	0.333	0.5	0.7	0.9
$\beta$	21.9	22.9	21.8	20.2

Environments, for which the probability of detection is calculated, take two categories; homogeneous and non-homogeneous, since the two environments differ in input array arrangement. The probabilities of detection versus signal to noise ratio (SNR) curves are plotted for the two environments. The plotted curve of probability of detection versus (SNR) at  $P_{fa} = 10^{-6}$  is shown in Fig. 7, where M represents the number of interference targets.

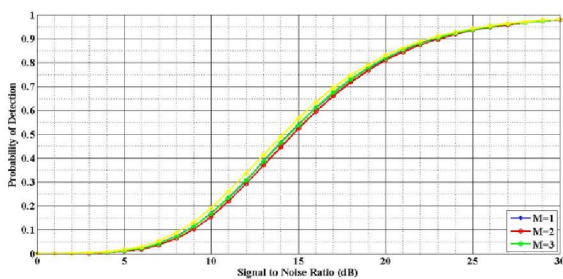


Fig. 7: Probability of detection of (IS-CFAR) – aided complex wavelet de-noising with homogeneous environment, swerling II case, and  $P_{fa} = 10^{-6}$ .

Fig.(7) shows that the three curves are coincides with each other approximately, which indicates that probability of detection of this system is independent on the number of targets, and the system can detect any number of targets with the same probability of detection. Also, this behavior is repeated by (IS-CFAR) – aided complex wavelet de-noising with  $\alpha = 0.7$  and  $\beta = 16$  as shown in Fig.8, for case non-homogeneous environment with swerling II and  $P_{fa} = 10^{-5}$ .

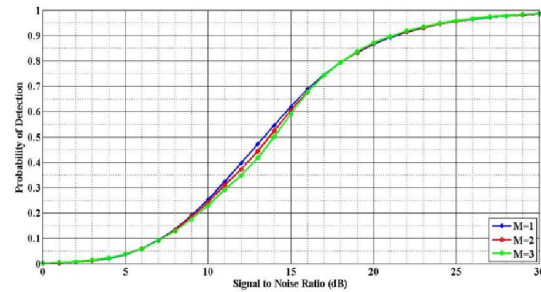


Fig. 8: Probability of detection of (IS-CFAR) – aided complex wavelet de-noising with non-homogeneous environment, swerling II case, and  $P_{fa} = 10^{-5}$ .

In homogeneous environment with swerling II case, the evaluation of the (IS-CFAR) – aided complex wavelet de-noising is deduced by make a comparison with (IS-CFAR) characteristic as shown in Fig.(9) and Fig.(10).

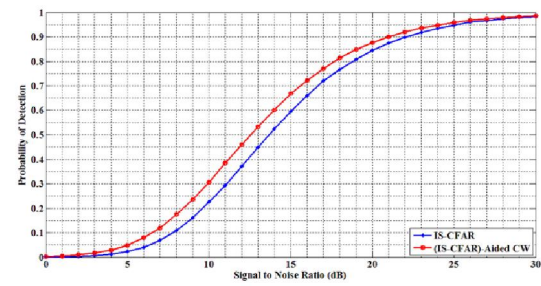


Fig. 9: Comparison in probability of detection with homogeneous environment, swerling II case,  $\alpha=0.5$  and  $P_{fa}=10^{-6}$

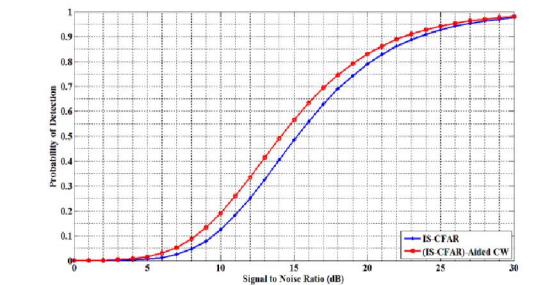


Fig. 10: Comparison in probability of detection with homogeneous environment, swerling II case,  $\alpha = 0.9$  and  $P_{fa} = 10^{-6}$ .

From Fig.(9) and Fig.(10), there is an improvement in SNR gain of approximately (1.2 dB) in all probability of detection range, which give good evaluation performance.

In homogeneous environment with swerling III case, the comparison of detection characteristic is plotted for  $\alpha = 0.5$  at  $P_{fa} = 10^{-5}$  and  $P_{fa} = 10^{-6}$  as shown in Fig.(11) and Fig.(12) respectively.

From Fig.(12), there is an excellent improvement in SNR gain of approximately (2.3 dB) in all probability of detection range.

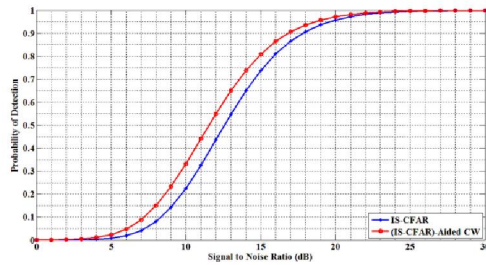


Fig. 11 : Comparison in probability of detection with homogeneous environment, swerling III case,  $\alpha = 0.5$  and  $P_{fa} = 10^{-5}$ .

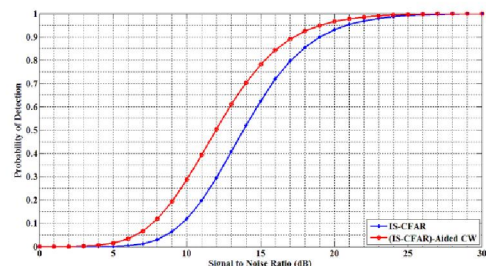


Fig. 12: Comparison in probability of detection with homogeneous environment, swerling III case,  $\alpha = 0.5$  and  $P_{fa} = 10^{-6}$ .

## 8. Conclusions

This paper shows the de-noising algorithm based upon the complex wavelet transform (CWT) that can be applied successfully to enhance noise removal, since it provided a considerable improvement in the probability of detection. Also, the proposed system presented similar probability of detection behavior for multiple number of targets ( $M$ ) case, since the targets (when  $M = 3$ ) have near probability of detection against SNR characteristics. The implementation of the (IS-CFAR) – aided CWT in the de-noising of reference cells has been examined. As shown by the experimental results for most of the de-noising applications the CWT gives better results than the classical wavelet transform. Since, in homogeneous environment with swerling II case, the probability of detection against SNR characteristic of (IS-CFAR) – aided CW de-noising outperforms characteristic of (IS-CFAR) for  $\alpha = 0.5$  at  $P_{fa} = 10^{-5}$  and  $\alpha = 0.9$  at  $P_{fa} = 10^{-6}$ . In homogeneous environment with swerling III case, the probability of detection against SNR characteristic of (IS-CFAR) – aided CW de-noising outperforms characteristic of (IS-CFAR) for  $\alpha = 0.5$  at both  $P_{fa} = 10^{-5}$  and  $P_{fa} = 10^{-6}$ .

## References

1. T. V. Cao (2012). Nonhomogeneity Detection in CFAR Reference Windows using the Mean – to – Mean Ratio

Test, published by DSTO – TR – 2608, AR No. AR-015-113.

2. James J. Jen (2011). "A Study of CFAR Implementation Cost and Performance Tradeoffs in Heterogeneous Environments", A master Thesis Presented to the Faculty of California State Polytechnic University, Pomona.
3. G. V. Weinberg (2004). Estimation of False Alarm Probabilities in Cell Averaging Constant False Alarm Rate Detectors via Monte Carlo Methods, published by DSTO – TR – 1624, AR No. AR-013-220.
4. G.A. Lampropoulosa, G. Giglia, A. ajjb and M. Rey (1998). "A New Adaptive Coherent CFAR Wavelet Detector" SPIE 1St. Clair Avenue West, Suite 1103 Toronto, Ontario, CANADA Vol. 3491 pp.1010-1016.
5. Z. Messalil, M. SahnoudP and F. Soltani (2005). Robust Detection of Distributed CACFAR in Presence of Extraneous Targets and Non-Gaussian Clutter, IEEE Electronic Departement, Constantine University, Algeria 2 TSI, Telecom-Paris, 3739, rue Dareau, 75014 Paris, France pp.547-550.
6. M. Alamdari, M. Modarres-Hashemi (2007). An Improved CFAR Detector Using Wavelet Shrinkage in Multiple Target Environments, IEEE Department of Electrical and Computer Engineering, Isfahan University of Technology, Isfahan, Iran.
7. Saeed Erfanian1, Vahid T. Vakili(2008). Analysis of Improved Switching CFAR in the Presence of Clutter and Multiple Targets, IEEE Electrical Engineering Department, Iran University of Science & Technology (IUST) Narmak 16846, Tehran, Iran PP.257-260.
8. Renli Zhang, Weixing Sheng n, Xiaofeng Ma (2013). Improved switching CFAR detector for non-homogeneous environments, ScienceDirect School of Electronic and Optoelectronic Engineering, Nanjing University of Science and Technology, Nanjing 210094, China, Signal Processing volume 93 issue 1 pp.35–48 J.
9. D. E. Newland(1994). An Introduction to Random Vibrations, Spectral and Wavelet Analysis. Longman Scientific & Technical, Essex, U.K. third edition.
10. Sheng-Tun Li, Shih-Wei Chou, and Jeng-Jong Pan (2000). Multi-resolution spatiotemporal data mining for the study of air pollutant regionalization. In 33rd Annual Hawaii International Conference on System Sciences (HICSS).
11. G. Beylkin, R. Coifman and V. Rokhlin(1991). Fast wavelet transforms and numerical algorithms, Communications on Pure and Applied Mathematics, pp. 141-183.
12. C. P. Bernard(1999). Discrete wavelet analysis for fast optic flow computation, Technical Report, Ecole Polytechnique.
13. M. Unser (1995). Texture classification and segmentation using wavelet frames, IEEE Transactions on Image Processing, Vol.4, pp. 1549-1560.
14. J. Neumann and G. Steidl(2003). Dual-Tree complex wavelet transform in the frequency domain and an application to signal classification, Technical Report, University of Mannheim.
15. D. L. Donoho(1995). De-noising by soft-thresholding, IEEE Transactions on Information Theory, Vol. 41, pp. 613-627.